JOURNAL OF CATALYSIS 70, 440–444 (1981)

Surface Interaction in the MoO_3/γ-Al_2O_3 System

In a recent review on the characterization of the molybdena catalysts (*1*), it was pointed out that the reducibility of a supported molybdena catalyst was often reported differently and much of the disparity may be due to the differences in catalyst preparation which include (i) the support used, (ii) mode of preparation, and (iii) calcination and other pretreatments. These factors may cause variation of dispersion and molybdena–support interaction which affect the reducibility of the supported MoO_3.

The dispersion of MoO_3 has been studied by (i) measuring the oxygen chemisorption at low temperature (78–195°K) on a prereduced molybdena (*2–4*), (ii) measuring the butene chemisorption at 100°C (*5*), and (iii) measuring the hydroxyls of the alumina (*6*). Monolayer dispersion of MoO_3 on γ-Al_2O_3 can be made by using an impregnation technique followed by calcination at 500°C (*7, 8*) or by adsorbing $MoO_2(OH)_2$ at 600°C from the gas phase (*9*). About 13–20 wt% MoO_3 can be deposited as a monolayer depending on the surface area of the support. Additional deposited MoO_3 then forms clusters. Upon heating in H_2 at 450–500°C, monolayer MoO_3 was reduced and shrunk to form an "interrupted monolayer" of MoO_2 or microcrystalline MoO_2 (*2, 10*).

This paper reports selective CO and NO chemisorption measurements on MoO_3 supported on γ-Al_2O_3 after reduction by H_2 at 500°C as a function of initial MoO_3 concentration. From these data the state of dispersion of MoO_3 on γ-Al_2O_3 can be found. It reports also the temperature-programmed reduction (TPR) of MoO_3, either pure or supported on γ-Al_2O_3, and these data are used to discuss the effects of dispersion and pretreatment on the reduction properties of MoO_3.

EXPERIMENTAL

The alumina support was made by agglomerating Dispal-M γ-Al_2O_3 powder (Continental Oil Company) and subsequently wetting, drying, and calcining at 600°C for 16 hr. The resulting solid mass was crushed and sieved. The 0.5 to 1.0-mm-diameter fraction (180 m^2/g BET area) was impregnated with $(NH_4)_2Mo_2O_7$ solution of a desired concentration, dried, and calcined in air at 400–600°C (Table 2) to form MoO_3 on γ-Al_2O_3. Research grade He, N_2, and CO were used without further purification. Hydrogen was purified by passage over an Engelhard Deoxo Pd catalyst and a 4A molecular sieve at 78°K. Nitric oxide was purified by repeated freezing–evaporation cycles, using only a portion of the middle fraction.

The apparatus and procedure used for the chemisorption measurement and the TPR by H_2 have been described in our previous paper (*11*).

The reproducibility of the data from chemisorption and TPR largely depends on the surface concentration of MoO_3 and the pretreatment of the sample. For example, without a reduction by H_2 at temperature >300°C, no irreversible chemisorption of either NO or CO is found (*12*). Reduction by H_2 and subsequent degassing at different temperature can also affect the chemisorption. In this work, all samples are reduced by flowing H_2 at 500°C for 1 hr before use. The standard deviation of chemisorption data is about 10%. Precalcination affects significantly the reproducibility of TPR data for the MoO_3/γ-Al_2O_3 samples of low Mo loading. Such effects are more pronounced

0021-9517/81/080440-05$02.00/0

for H_C/Mo values at 500°C than for H_C/Mo values at 900°C (Table 2). The standard deviation of H_C/Mo at 500°C of low Mo loading can reach about 15%, while that of H_C/Mo at 900°C is significantly smaller (4%).

RESULTS AND DISCUSSION

1. Chemisorption Measurements

CO and NO can chemisorb irreversibly on MoO_3/γ-Al_2O_3 at 25°C after the material is reduced by H_2 at 500°C (*12*). Typical adsorption isotherms of NO and CO at 25°C on MoO_3/γ-Al_2O_3 reduced by H_2 and degassed at 500°C for 1 hr are presented in Fig. 1. Similar to Ref. (*15*), curves A and B give, respectively, the total and reversible adsorption, and curve C the irreversible part. The reversible part is measured following the total adsorption after the same sample is degassed at 25°C for $\frac{1}{2}$ hr.

The dispersion of MoO_3 on γ-Al_2O_3 is examined by selective CO and NO chemisorption as a function of Mo loading. A logarithmic plot of irreversible CO and NO uptake vs Mo loading is shown in Fig. 2. For samples of low Mo loading, both NO and CO chemisorptions increase logarithmically with Mo loading until a given concentration of Mo is reached. Then the increase of uptakes virtually stops. The saturation concentration of MoO_3 in the dispersed phase is indicated by the intersection of the two lines and corresponds to about 4.0 μmol Mo/m^2 (BET). This saturation concentration of MoO_3 on γ-Al_2O_3 is much higher than that of Re (*11*), Rh (*13*), and Pt (*14*) oxides on γ-Al_2O_3 (2.0–2.5 μmol/m^2 (BET) but is considerably lower than that of Co_3O_4 on ZrO_2 (7.6 μmol/m^2 (BET) (*15*). When the Mo loading is beyond this saturation concentration, the excess MoO_3 aggregates to form a particulate or bulk phase and both CO and NO chemisorptions level off.

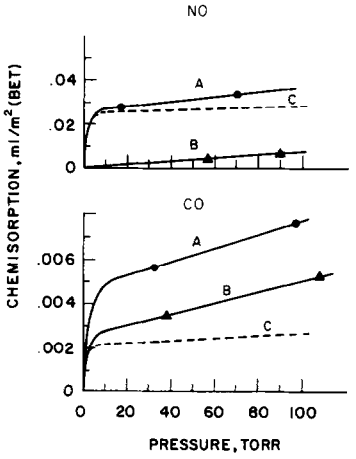

FIG. 1. Adsorption isotherms of CO and NO at 25°C on MoO_3/γ-Al_2O_3 (2.9 wt% Mo, reduced at 500°C): A, total adsorption; B, reversible part; C, irreversible part.

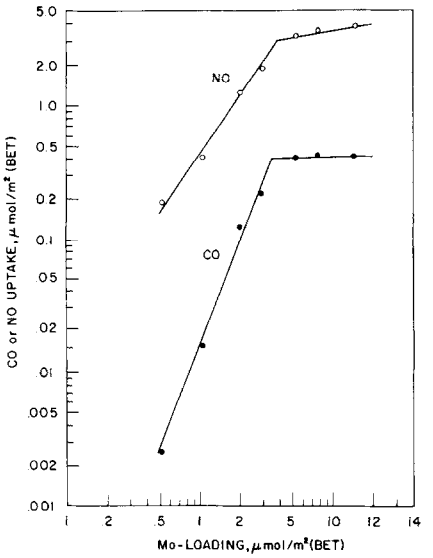

FIG. 2. Irreversible NO and CO uptake as a function of Mo loading.

Stoichiometries of the irreversible NO and CO chemisorptions on reduced MoO_3/γ-Al_2O_3 samples, NO/Mo and CO/Mo, are given in Table 1. The results indicate that NO/Mo values vary with Mo concentration and are much higher than the corresponding CO/Mo values. We attribute this large difference between NO/Mo and CO/Mo values to the much stronger chemisorption of NO than that of CO on the reduced Mo oxide. It was often observed previously that the chemisorption of NO on

TABLE 1

Irreversible Chemisorption of NO and CO on $Mo/\gamma\text{-}Al_2O_3$

Samples	Mo loading		NO (μmol/m^2(BET))	NO/Mo	CO (μmol/m^2(BET))	CO/Mo
	wt% Mo	μmol/m^2(BET)				
1	0.75	0.53	0.18	0.34	0.0026	0.005
2	1.50	1.06	0.39	0.37	0.016	0.015
3	2.86	2.00	1.24	0.62	0.125	0.063
4	4.07	2.95	1.85	0.63	0.22	0.075
5	7.19	5.22	3.25	0.62	0.41	0.078
6	10.10	7.80	3.40	0.45	0.42	0.055
7	18.24	14.2	3.75	0.26	0.41	0.029

transition metal oxide can be much stronger than the chemisorption of CO and that a lower pressure is sufficient to obtain a monolayer coverage in the case of NO. For supported Mo oxide, this difference is more pronounced (*12*). The much weaker CO chemisorption is indicated here by the relatively large amount of reversible adsorption of CO compared to that of NO (Fig. 1). On the other hand, the much stronger NO chemisorption has been shown in an ir study (*16*) in which NO molecules are doubly adsorbed at room temperature and desorbed only at 200–300°C to yield N_2O. Even though the NO chemisorption is strong and doubly adsorbed, the stoichiometries of NO/Mo (Table 1) remain much lower than unity. It was reported (*17, 18*) that when the reduction of $MoO_3/\gamma\text{-}Al_2O_3$ reached the stage of $H_C/Mo = 2$, approximately 75% of Mo^{6+} are converted to Mo^{4+} and only about 17% of these Mo^{4+} ions are active sites for NO chemisorption. This will give a NO/Mo ratio of 0.28 if NO is singly adsorbed or a ratio of 0.56 if it is doubly adsorbed. The latter is closer to the NO/Mo values in Table 1.

Both NO/Mo and CO/Mo values (Table 1) decrease with Mo loading in the dispersed phase and CO/Mo value decreases faster than NO/Mo value. This decrease of adsorptive activity is consistent with the decrease of reducibility of MoO_3 at 500°C and is interpreted as due to the increase of MoO_3–support interaction in the dispersed phase (see below).

2. TPR

The rates of hydrogen uptake as a function of temperature in the TPR of pure MoO_3 and MoO_3 supported on $\gamma\text{-}Al_2O_3$ at various MoO_3 concentrations are presented in Fig. 3. These data allow a direct comparison of the reduction of pure MoO_3 (curve A) with that of MoO_3 supported on $\gamma\text{-}Al_2O_3$ at various MoO_3 concentrations (curves B, C, and D). In these reductions, the temperature was increased at a rate of 10°C per minute and then was maintained at 900°C for an hour. Three rate maxima appeared in all curves except curve D which has only two. In a separate experiment, where the reduction temperature was increased and was maintained at 500°C for an hour, incomplete reductions of MoO_3 were found. A complete reduction can be reached by increasing temperature to 900°C. These results are summarized in Table 2. The appearance of multiple rate maxima in Fig. 3 indicates the difference in the ease of hydrogen consumption at the different stages of reduction.

It has been suggested (*17*) that Mo^{6+} ions in $MoO_3/\gamma\text{-}Al_2O_3$ of low Mo loading (<8 wt% Mo) are distributed in two different alumina sites: a nonreducible tetrahedral site, Mo(T), and a reducible octahedral site, Mo(O). The concentration ratio of Mo(O)

to Mo(T) is low when Mo loading is low but increases with Mo surface concentration. The mechanism of reduction by H_2 at 500°C for the γ-Al_2O_3-supported MoO_3 was postulated (*18*, *19*) in the following:

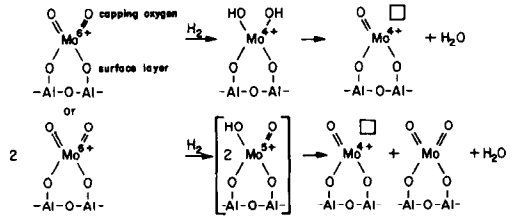

On the basis of this mechanism, one can assume that the ease of reduction at 500°C depends on the surface concentration of the capping oxygen, surface structure of MoO_3 in the dispersed phase, and surface amorphousness in the bulk phase. For pure MoO_3 powder, the BET areas are low and H_C/Mo values at 500°C are small (Table 2). Higher H_C/Mo values were reported for bulk MoO_3 obtained from the decomposition of $(NH_4)_6Mo_7O_{24}$ (*5*). For the γ-Al_2O_3-supported MoO_3 samples, the reduction rate and H_C/Mo values at 500°C are higher. A maximum value of $H_C/Mo = 2$ at 500°C is found for samples of high Mo loading (Table 2). Prolonged calcination at 400 and 500°C does not affect H_C/Mo values for samples of high Mo loading but lowers significantly the H_C/Mo values at 500°C for samples of low Mo loading. This effect of heat treatment on the reducibility at 500°C can be attributed to the increase of the MoO_3–support interaction in the dispersed phase which may lower the surface concentration of the capping oxygen and

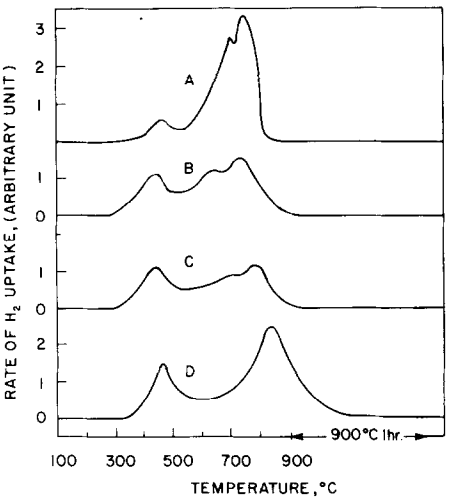

FIG. 3. Rate of hydrogen uptake as a function of temperature in the TPR of (A) pure MoO_3 (Baker-analyzed reagent, J. T. Baker Chemical Company); (B) 10.1 wt% Mo/γ-Al_2O_3; (C) 7.2 wt% Mo/γ-Al_2O_3; (D) 2.9 wt% Mo/γ-Al_2O_3.

TABLE 2

Average Hydrogen Consumption per Molybdenum, H_C/Mo, at 500 and 900°C

Sample	BET area, (m^2/g)	Calcination in air		H_C/Mo (500°C, 1 hr)	H_C/Mo (900°C, 1 hr)
		Temperature	Time		
MoO_3 powder (A)[a]	0.63	500	3	0.3	6.0
MoO_3 powder (B)[a]	1.46	500	20	0.8	6.0
10.1 wt% Mo/γ-Al_2O_3	135	400	4	2.0	6.0
10.1 wt% Mo/γ-Al_2O_3	135	500	20	2.1	6.0
2.86 wt% Mo/γ-Al_2O_3	146	400	2	1.6	6.2
2.86 wt% Mo/γ-Al_2O_3	146	500	20	0.5	6.0
1.5 wt% Mo/γ-Al_2O_3	148	400	2	1.2	6.1
1.5 wt% Mo/γ-Al_2O_3	148	500	20	0.4	5.8
1.5 wt% Mo/γ-Al_2O_3	148	600	2	0.15	5.5

[a] MoO_3 (A) is the Baker-analyzed reagent, J. T. Baker Chemical Company.

[b] MoO_3 (B) is the decomposition product of ammonium dimolybdate (experimental chemical, Climax Molybdenum Company).

the concentration ratio of Mo(O)/Mo(T) in the dispersed phase (*17*).

After the reduction at 500°C, the oxygen atoms in the surface layer and in the bulk can be removed further at higher temperatures (shown as the second and the third rate maxima in curves A, B and C in Fig. 3). For MoO_3/γ-Al_2O_3 of low Mo loading, the reduction at 500°C left only the oxygen atoms of MoO_3 in the surface layer which can be removed at about 850°C (curve D in Fig. 3).

ACKNOWLEDGMENTS

The author acknowledges many helpful discussions with Drs. M. Shelef, H. S. Gandhi, and M. Bettman.

REFERENCES

1. Massoth, F. E., *in* "Advances in Catalysis," Vol. 27, p. 265. Academic Press, New York/London, 1978.
2. Parekh, B. S., and Weller, S. W., *J. Catal.* **47,** 100 (1977).
3. Millman, W. S., and Hall, W. K., *J. Catal.* **59,** 311 (1979).
4. Fierro, J. L. G., Mendioroz, S. Pajares, J. A., and Weller, S. W., *J. Catal.* **65,** 263 (1980).
5. Massoth, F. E., *J. Catal.* **30,** 204 (1973).
6. Fransen, T., van der Meer, O., and Mars, P., *J. Catal.* **42,** 79 (1976).
7. Giordano, N., Bart, J. C. J., Vaghi, A., Castellan, A., and Martinotti, G., *J. Catal.* **36,** 81 (1975).
8. Giordano, N., Castellan, A., Bart, J. C. J., Vaghi, A., and Campadelli, F., *J. Catal.* **37,** 204 (1975).
9. Sonnemans, J., and Mars, P., *J. Catal.* **31,** 209 (1973).
10. Schuit, G. C. A., and Gates, B. C., *Amer. Inst. Chem. Eng. J.* **19,** 417 (1973).
11. Yao, H. C., and Shelef, M., *J. Catal.* **44,** 392 (1976).
12. Lombardo, E. A., Lo Jacono, M., and Hall, W. K., *J. Catal.* **64,** 150 (1980).
13. Yao, H. C., Japar, S., and Shelef, M., *J. Catal.* **50,** 407 (1977).
14. Yao, H. C., Sieg, M., and Plummer, H. K., Jr., *J. Catal.* **59,** 365 (1979).
15. Yao, H. C., and Bettman, M., *J. Catal.* **41,** 349 (1976).
16. Millman, W. S., and Hall, W. K., *J. Phys. Chem.* **83,** 427 (1979).
17. Chung, K. S., and Massoth, F. E., *J. Catal.* **64,** 320 (1980).
18. Hall, W. K., and Lo Jacono, M., *in* "Proceedings, 6th International Congress on Catalysis, London, 1976" (G. C. Bonds, P. B. Wells, and F. C. Tompkins, Eds.), Vol. 1, p. 246. The Chemical Society, London, 1977.
19. Hall, W. K., and Massoth, F. E., *J. Catal.* **34,** 41 (1974).

H. C. YAO

Engineering & Research Staff
Ford Motor Company
Dearborn, Michigan 48121

Received June 30, 1980; revised January 27, 1981